Topological phases in the presence of disorder and longer-range couplings

Gianluca Francica, Edoardo Maria Tiburzi, and Luca Dell'Anna
Dipartimento di Fisica e Astronomia G. Galilei, Università degli Studi di Padova, via Marzolo 8, 35131 Padova, Italy

(Received 18 December 2022; revised 25 March 2023; accepted 4 April 2023; published 20 April 2023)

We study the combined effects of disorder and range of the couplings on the phase diagram of one-dimensional topological superconductors. We consider an extended version of the Kitaev chain where hopping and pairing terms couple many sites. Deriving the conditions for the existence of Majorana zero modes, we show that either the range and the on-site disorder can greatly enhance the topological phases characterized by the appearance of one or many Majorana modes localized at the edges. We consider both a discrete and a continuous disorder distribution. Moreover, we discuss the role of correlated disorder which might further widen the topological regions. Finally, we show that in the purely long-range regime and in the presence of disorder, the spatial decay of the edge modes remains either algebraic or exponential, with eventually a modified localization length, as in the absence of disorder.

DOI: 10.1103/PhysRevB.107.165137

I. INTRODUCTION

Topological materials can exhibit boundary modes, topologically protected if the symmetries of the system are not broken [1,2]. A so-called bulk-boundary correspondence relates the existence of these boundary modes to the topology of the quantum phase which is fully characterized by bulk topological invariants. The Kitaev one-dimensional chain [3] is a paradigmatic model exhibiting a topologically nontrivial quantum phase with two Majorana zero modes (MZMs) localized at the edges. Experimental realizations of such topological superconductors employ one-dimensional arrays of magnetic impurities [4–6] or semiconducting nanowires [7–10] on top of a conventional superconducting substrate. MZMs are of some importance for achieving full-scale quantum computation. Actually, they were originally proposed with the aim to realize a quantum register immune from decoherence [11,12]. Theoretically, this goal should be achievable due to the possibility of fault-tolerant quantum computation which can be obtained at the physical level instead of using quantum error-correcting codes. The Kitaev chain is a way of constructing decoherence-protected degrees of freedom in one-dimensional systems. The question whether topological properties, exhibited by this model, are affected by longer-range couplings or randomness, all phenomena which might occur in real experimental setups, are therefore of some relevance. Several studies have been performed to understand the effects on the MZMs of long-range couplings [13–16], where bulk-boundary correspondence is still under investigation [16–18], the effects of disorder [19–31] and interactions [24,32–36], by considering several setups for experimental realizations [37–55]. Fermionic chains have also been examined in the presence of next-nearest-neighbor couplings [56] and long-range pairing with incommensurate potentials [57]. In this paper, we aim at investigating the combined effect of disorder and longer-distance couplings on the topological phase diagrams, considering a chain of fermions which can host one or many couples of MZMs at the edges. In the absence of disorder, the effect of longer-range couplings has been investigated in Ref. [14]. On the other hand, the effect of uniform disorder, for the Kitaev chain with nearest neighbor couplings, has been studied in Ref. [24]. We will show, both numerically and analytically, that the combined effect of disorder and range of the couplings is that of promoting the topological phases, increasing both their number and their extension, concluding that these elements, occurring in the real experimental realizations of the model, can even better stabilize the topological order. Finally, we note that longer-range chains can be related to multichannel topological superconductors (see, e.g., Ref. [58]), where the role of disorder has also been investigated [59–62]. In particular, some positive effects of weak disorder have been originally observed in the case of multichannel [45] and multiband [63] topological superconductors.

II. MODEL

To study the interplay between the interaction range and the strength of an on-site disorder, we consider the extended version of the Kitaev chain, taking into account r neighbor couplings in the hopping and pairing terms, as done in Ref. [14], with local random energies μ_j. This model is described by the following Hamiltonian:

$$H = -\sum_{\ell=1}^{r}\sum_{j=1}^{L-\ell}(w_\ell a_j^\dagger a_{j+\ell} - \Delta_\ell a_j a_{j+\ell} + \text{H.c.}) + \sum_{j=1}^{L}\mu_j\left(a_j^\dagger a_j - \frac{1}{2}\right), \tag{1}$$

where a_j ($a_j^\dagger$) annihilates (creates) a fermion in the site j, μ_j is the space-dependent chemical potential, w_ℓ is the hopping amplitude, and Δ_ℓ is the superconducting pairing. We can define the following Majorana operators: $c_{2j-1} = a_j + a_j^\dagger$ and $c_{2j} = -i(a_j - a_j^\dagger)$, such that $\{c_i, c_j\} = 2\delta_{i,j}$. The Hamiltonian

in Eq. (1) can be rewritten as

$$H = -\frac{i}{2}\sum_{j=1}^{L}\mu_j c_{2j-1}c_{2j} + \frac{i}{2}\sum_{\ell=1}^{r}(w_\ell+\Delta_\ell)\sum_{j=1}^{L-\ell}c_{2j}c_{2j+2\ell-1} - \frac{i}{2}\sum_{\ell=1}^{r}(w_\ell-\Delta_\ell)\sum_{j=1}^{L-\ell}c_{2j-1}c_{2j+2\ell}. \quad (2)$$

The model belongs to the BDI class and can exhibit a positive number of MZMs per edge. The case of a homogeneous chemical potential $\mu_j = \mu$ has been extensively studied in Ref. [14], where, to find the Majorana modes, a general transfer matrix approach has been introduced.

A recent proposal for realizing a BDI topological superconductor from a AIII topological insulator is reported in Ref. [64]. The first experimental proposal [7–9], instead, makes use of a quantum wire put in proximity of an s -wave superconductor in the presence of spin-orbit coupling and magnetic field, which generate a topological superconductor of class D. In this latter case, the BDI class can be reached in the limit of strong magnetic field compared to the spin-orbit coupling.

A. Transfer matrix

The transfer matrix approach can be easily generalized to the case of an inhomogeneous chemical potential. We will consider the presence of disorder, so μ_j is randomly distributed. To determinate whether MZMs exist, we look for a MZM of the form $b_1 = \sum_{j=1}^{L}\psi_j c_{2j}$. The condition $[H, b_1] = 0$ is satisfied if

$$\sum_{\ell=1}^{r}(w_\ell+\Delta_\ell)\psi_{i-\ell} - \sum_{\ell=1}^{r}(w_\ell-\Delta_\ell)\psi_{i+\ell} + \mu_i\psi_i = 0, \quad (3)$$

so the mode is localized at one edge, after imposing r boundary conditions ($\psi_i = 0$ for $-r < i \leqslant 0$ or $L < i \leqslant L+r$). One can find an analogous condition for the zero mode at the other edge, which reads

$$\sum_{\ell=1}^{r}(w_\ell+\Delta_\ell)\phi_{i+\ell} - \sum_{\ell=1}^{r}(w_\ell-\Delta_\ell)\phi_{i-\ell} + \mu_i\phi_i = 0 \quad (4)$$

after requiring $[H, b_2] = 0$, with $b_2 = \sum_{j=1}^{L}\phi_j c_{2j-1}$, and imposing r boundary conditions ($\phi_i = 0$ for $L < i \leqslant L+r$ or $-r < i \leqslant 0$). In particular, Eq. (4) can be expressed as

$$\vec{\Phi}_{i+1} = \mathcal{A}_i\vec{\Phi}_i, \quad (5)$$

where $\vec{\Phi}_i = (\phi_{i+r-1}, \phi_{i+r-2}, \cdots, \phi_i, \cdots, \phi_{i-r})^T$, and $\mathcal{A}_i$ is the transfer matrix

$$\mathcal{A}_i = \begin{pmatrix} t_1 & t_2 & \cdots & t_{2r-1} & t_{2r} \\ 1 & 0 & \cdots & 0 & 0 \\ 0 & 1 & \cdots & 0 & 0 \\ \vdots & \vdots & \ddots & \vdots & \vdots \\ 0 & 0 & \cdots & 1 & 0 \end{pmatrix}, \quad (6)$$

where $t_\ell = -\frac{\Delta_{r-\ell}+w_{r-\ell}}{\Delta_r+w_r}$ for $1 \leqslant \ell < r$, $t_r = -\frac{\mu_i}{\Delta_r+w_r}$ and $t_\ell = \frac{\Delta_{\ell-r}-w_{\ell-r}}{\Delta_r+w_r}$ for $r < \ell \leqslant 2r$. By considering the eigenvalues of the matrix $\tilde{\mathcal{A}}_n$, defined as

$$\tilde{\mathcal{A}}_n = \mathcal{A}_n\mathcal{A}_{n-1}\cdots\mathcal{A}_2\mathcal{A}_1, \quad (7)$$

we get a number $N = \max(v^>, v^<) - r$ of MZMs, where $v^>$ and $v^<$ are the numbers of eigenvalues λ_n that diverge and tend to zero as $n \to \infty$ (see Ref. [14] for details).

For $w_\ell = \Delta_\ell$, the condition expressed in Eq. (4) reduces to $2\sum_{\ell=1}^{r} w_\ell\phi_{i+\ell} + \mu_i\phi_i = 0$, which can be expressed as

$$\vec{\phi}_{i+1} = A_i\vec{\phi}_i, \quad (8)$$

where now $\vec{\phi}_i = (\phi_{i+r-1}, \phi_{i+r-2}, \cdots, \phi_i)^T$, and A_i is the transfer matrix

$$A_i = \begin{pmatrix} t_1 & t_2 & \cdots & t_{r-1} & t_r \\ 1 & 0 & \cdots & 0 & 0 \\ 0 & 1 & \cdots & 0 & 0 \\ \vdots & \vdots & \ddots & \vdots & \vdots \\ 0 & 0 & \cdots & 1 & 0 \end{pmatrix}. \quad (9)$$

where $t_\ell = -\frac{w_{r-\ell}}{w_r}$ for $\ell = 1, \ldots, r-1$, and $t_r = -\frac{\mu_i}{2w_r}$. Indeed, for $w_\ell = \Delta_\ell$,

$$\mathcal{A}_i = \begin{pmatrix} A_i & 0 \\ \Sigma_+ & \Sigma_- \end{pmatrix}, \quad (10)$$

where Σ_+ is a $r \times r$ matrix with all entries equal to zero except the right-top element equal to 1, while Σ_- is a $r \times r$ matrix with all entries equal to zero except $(r-1)$ elements along the low diagonal, below the main diagonal, which are equal to 1. Actually Σ_- does not play any role since it gives trivial identities. As a result,

$$\tilde{\mathcal{A}}_n = \begin{pmatrix} \tilde{A}_n & 0 \\ \cdots & \Sigma_-^n \end{pmatrix}, \quad (11)$$

where, analogously to Eq. (7), we define

$$\tilde{A}_n = A_nA_{n-1}\cdots A_2A_1, \quad (12)$$

and for large distances, $n \geqslant r$, we have $\Sigma_-^n = 0$.

Finally, for an infinite range, $r \to \infty$, and an algebraic decay of the couplings, $w_\ell = w/\ell^\alpha$ and $\Delta_\ell = \Delta/\ell^\beta$, for α and $\beta > 1$, we can have only zero or one MZM, algebraically localized at each edge or exponentially localized for $w_\ell = \Delta_\ell$ [65,66].

III. NEAREST-NEIGHBOR COUPLINGS ($r = 1$)

The case of nearest neighbor coupling, $r = 1$, has been investigated in Ref. [24]. For $w \neq \Delta$, we get the transfer matrix

$$\mathcal{A}_i = \begin{pmatrix} -\frac{\mu_i}{\Delta+w} & \frac{\Delta-w}{\Delta+w} \\ 1 & 0 \end{pmatrix}, \quad (13)$$

thus there is one MZM per edge if $v^> = 2$ or $v^< = 2$.

For the case $w_1 = \Delta_1$, from Eq. (4) we get $\phi_{i+1} = m_i\phi_i$, from which

$$\phi_{n+1} = \phi_1\prod_{i=1}^{n} m_i, \quad (14)$$

where we defined

$$m_i \equiv -\frac{\mu_i}{2w}. \quad (15)$$

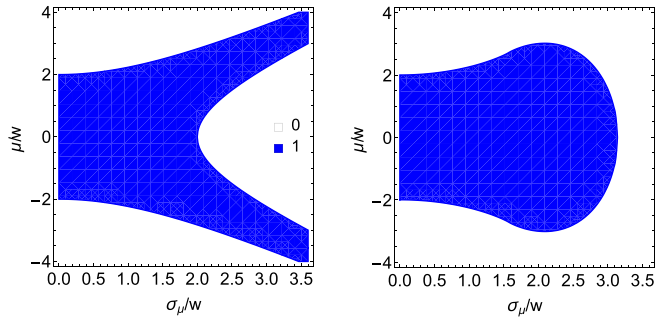

FIG. 1. Topological phase diagrams σ_μ-μ, for $r = 1$ and $w = \Delta$, where μ and σ_μ^2 are, respectively, the mean value and the variance of the distribution of the random variables μ_i. The blue regions are characterized by one MZM, while the white regions are trivial, with zero MZMs, for two different distributions of the disorder: bimodal (left) and uniform box (right) distributions.

The only nonzero eigenvalue of the transfer matrix product is $\lambda = \prod_{i=1}^n m_i$, which is equal to $\tilde{A}_n$. Let us now rewrite the absolute value of ϕ_{n+1} as follows:

$$|\phi_1| \prod_{i=1}^{n} |m_i| = |\phi_1| \exp\left[\sum_{i=1}^{n} \ln |m_i|\right] = |\phi_1| e^{n\langle \ln |m_i|\rangle}. \quad (16)$$

In the thermodynamic limit, the topological phase is determined by the behavior of the mean logarithm $\langle \ln |m_i|\rangle \equiv \sum_{i=1}^n \ln |m_i|/n$, for large n, if this quantity is negative, the eigenvalue λ vanishes and a topological phase is allowed, otherwise the phase is trivial, i.e., there is one MZM per edge if

$$\langle \ln |m_i|\rangle < 0. \quad (17)$$

This condition can be fixed for any probability distribution of the random variables.

For instance, for a bimodal distribution, for which m_i can have only two values, $m_+ = m + \epsilon$ and $m_- = m - \epsilon$, with the same probability, so the probability distribution is $\frac{1}{2}\delta(m - m_+) + \frac{1}{2}\delta(m - m_-)$. The topological phase is, then, bounded by the solution of the following equation:

$$\tfrac{1}{2}(\ln |m + \epsilon| + \ln |m - \epsilon|) = 0. \quad (18)$$

Strikingly, for this special situation the topological phase extends indefinitely, even for large disorder, as far as $m \simeq \mp\epsilon$, namely, for $\mu \simeq \pm\sigma_\mu$, where μ is the mean value and σ_μ^2 the variance of the distribution of μ_i. At the band center, $\mu = 0$, the topological phase closes at $\epsilon = 1$, i.e., $\sigma_\mu = 2w$ (see Fig. 1).

Another example is the box distribution [24], when m_i are uniformly distributed in the interval $[m - \epsilon, m + \epsilon]$. We get a topological phase boundary solving the equation $\langle \ln |m_i|\rangle = 0$ which, in the continuum, reads $\frac{1}{2\epsilon}\int_{m-\epsilon}^{m+\epsilon} dm' \ln |m'| = 0$, or more explicitly,

$$\frac{m + \epsilon}{2\epsilon} \ln |m + \epsilon| - \frac{m - \epsilon}{2\epsilon} \ln |m - \epsilon| - 1 = 0. \quad (19)$$

This analytical condition gives the boundary for the topological phase in terms of the mean chemical potential $\mu/w = 2m$ and of the square root of the variance $\sigma_\mu/w = 2\epsilon/\sqrt{3}$ for a uniform distribution, reported in Fig. 1. The plot shows a peculiar behavior of the response of the system to the presence of disorder. As the strength of the disorder increases, the topological phase becomes wider and wider up to an optimal value beyond which it is suppressed and then disappears at $\sigma_\mu/w = 2e/\sqrt{3}$. For $w \neq \Delta$, the behavior of the topological phase is qualitatively the same, and is simply more or less extended depending on whether $|\Delta| > |w|$ or vice versa. Also, the normal distribution gives the same qualitative behavior.

We plan to generalize this study for a longer range of the couplings, $r > 1$ to investigate the combined effects of disorder and long-range couplings.

IV. NEXT-NEAREST-NEIGHBOR COUPLINGS ($r = 2$)

Let us now consider a range $r = 2$, namely, involving the nearest- and next-nearest-neighbor couplings. For simplicity, we will mainly focus on $w_\ell = \Delta_\ell$. The case of larger r shares similar features of the case $r = 2$, so we will also investigate the next-nearest neighbor in more detail because it is simpler from an analytical point of view.

First, let us consider the case with $w_1 = 0$ and $w_2 \neq 0$. From Eq. (4), we get

$$\phi_{i+2} + \frac{\mu_i}{2w_2}\phi_i = 0, \quad (20)$$

from which we obtain two equations for $i_0 = 1, 2$,

$$\phi_{2n+i_0} = \prod_{i=0}^{n-1} \left(-\frac{\mu_{2i+i_0}}{2w_2}\right) \phi_{i_0}, \quad (21)$$

which generalizes Eq. (14). So, similarly to what is done for $r = 1$, we now have two copies of the condition for getting one MZM,

$$\left\langle \ln \left| \frac{\mu_i}{2w_2} \right| \right\rangle_{i_0} < 0, \quad (22)$$

where we define the averages $\langle x_i\rangle_{i_0} = 2\sum_{i=0}^{n-1} x_{2i+i_0}/n$, valid for large n. If locally the distribution probability of the disorder is the same at any site, the two conditions in Eq. (22) (with $i_0 = 1$ and 2) are equal, and we can get only zero or two MZMs per edge.

In contrast, things change drastically if also the coupling $w_1 \neq 0$. Let us start considering the case $w_1 = w_2 = w$, so the transfer matrix reads

$$A_i = \begin{pmatrix} -1 & m_i \\ 1 & 0 \end{pmatrix}. \quad (23)$$

To determinate the eigenvalues λ_n of $\tilde{A}_n$, we consider the eigenvalue equation

$$\lambda_n^2 - \lambda_n \mathrm{Tr}(\tilde{A}_n) + \det(\tilde{A}_n) = 0. \quad (24)$$

Using the property of the determinant of a matrix product, we have simply

$$\det(\tilde{A}_n) = \prod_{i=1}^{n} \det(A_i) = (-1)^n \prod_{i=1}^{n} m_i, \quad (25)$$

and taking the absolute value we can write

$$|\det(\tilde{A}_n)| = \prod_{i=1}^{n} |m_i| = e^{n\langle \ln |m_i|\rangle} \quad (26)$$

as $n \to \infty$. The calculation of the trace is slightly more involved. As shown in Appendix A, we get

$$|\mathrm{Tr}(\tilde{A}_n)| \simeq e^{n\langle \ln |R_i| \rangle}, \tag{27}$$

as $n \to \infty$, where we define the random continued fraction

$$R_i = 1 + \cfrac{m_i}{1 + \cfrac{m_{i-1}}{1 + \cfrac{m_{i-2}}{1 + \ddots}}}, \tag{28}$$

which is the solution of the following recursive equation:

$$R_i = 1 + \frac{m_i}{R_{i-1}}. \tag{29}$$

We note that the mean values $\langle \ln |m_i| \rangle$ and $\langle \ln |R_i| \rangle$ can be evaluated by using the probability distributions of the random variables m_i and of the convergents R_i. Unlike the determinant, the trace depends on disorder in a nontrivial way. As shown in Appendix A, the trace reads

$$\mathrm{Tr}(\tilde{A}_n) \approx 1 + n\langle m_i \rangle + \frac{n^2}{2}\langle m_i \rangle^2 - \frac{n}{2}\langle m_i^2 \rangle - n\,\langle m_i m_{i-1} \rangle + \cdots, \tag{30}$$

where we neglected terms depending on higher moments and correlations. Clearly, the topological quantum phases can depend on both moments (e.g., $\langle m_i^2 \rangle$) and correlations (e.g., $\langle m_i m_{i-1} \rangle$) of the random variables. As a result, we expect that correlated and uncorrelated disorder can affect differently the topological phases. This behavior has to be contrasted to the case with $w_1 = 0$ where correlations do not play any role.

To derive the conditions for the existence of MZMs, for $w_\ell = \Delta_\ell$ we have to analyze the eigenvalue equation, Eq. (24). If $\det(\tilde{A}_n) \to 0$ or $\det(\tilde{A}_n)/\mathrm{Tr}(\tilde{A}_n) \to 0$, from Eq. (24) we get $\lambda_n(\lambda_n - \mathrm{Tr}(\tilde{A}_n)) \to 0$ or $\lambda_n(\lambda_n/\mathrm{Tr}(\tilde{A}_n) - 1) \to 0$, thus in both cases there is at least one eigenvalue that tends to zero, so there is at least one MZM per edge. If $\mathrm{Tr}(\tilde{A}_n) \to 0$ and $\det(\tilde{A}_n) \to 0$, for $n \to \infty$, from Eq. (24) we get $\lambda_n \to 0$, thus both the two eigenvalues go to zero, so there are two MZMs per edge. In summary, we get the following conditions:

$$\det(\tilde{A}_n) \to 0 \ \text{ or } \ \frac{\det(\tilde{A}_n)}{\mathrm{Tr}(\tilde{A}_n)} \to 0 \Rightarrow \exists\, 1 \text{ MZM}, \tag{31}$$

$$\det(\tilde{A}_n) \to 0 \ \text{ and } \ \mathrm{Tr}(\tilde{A}_n) \to 0 \Rightarrow \exists\, 2 \text{ MZMs}. \tag{32}$$

For $w_1 = w_2 = w$, using Eqs. (26) and (27), we get

$$\langle \ln |m_i| \rangle < 0 \ \text{ or } \ \langle \ln |m_i| \rangle < \langle \ln |R_i| \rangle \Rightarrow \exists\, 1 \text{ MZM}, \tag{33}$$

$$\langle \ln |m_i| \rangle < 0 \ \text{ and } \ \langle \ln |R_i| \rangle < 0 \ \Rightarrow \exists\, 2 \text{ MZMs}. \tag{34}$$

We now proceed in studying these conditions for the homogeneous case and then applying them to the cases of uncorrelated and correlated disorder.

A. Homogeneous case

Let us warm up considering first the clean system, namely, in the absence of disorder, always in the simplest case where $w_1 = w_2 = \Delta_1 = \Delta_2 \equiv w$. In this case, $m_i = m = -\mu/(2w)$ for any i, so we get

$$\det(\tilde{A}_n) = (-1)^n m^n, \tag{35}$$

$$\mathrm{Tr}(\tilde{A}_n) = \frac{(-1)^n}{2^n}[(1 + \sqrt{1 + 4m})^n + (1 - \sqrt{1 + 4m})^n]. \tag{36}$$

For $n \to \infty$, we get $\frac{\det(\tilde{A}_n)}{\mathrm{Tr}(\tilde{A}_n)} \to 0$ for $m \in (-1, 2)$ so, according to Eq. (31), we have at least one MZM per edge for $\mu/w \in (-4, 2)$. Moreover, $\mathrm{Tr}(\tilde{A}_n) \to 0$ for $m \in (-1, 0)$, so, using Eq. (32), we get two MZMs for $\mu/w \in (0, 2)$. These results are in perfect agreement with what reported in Ref. [14].

Let us redo the calculation using Eqs. (33) and (34), introducing the distribution $\rho(R_i)$ for a continued fraction, which will be useful also in the presence of disorder. For $m > -1/4$, we get $R_n \to \bar{R} = \frac{1}{2}(1 + \sqrt{1 + 4m})$ for $n \to \infty$, so $\rho(R_i) = \delta(R_i - \bar{R})$. To determinate the distribution $\rho(x)$ for $m < -1/4$, we consider the Frobenius-Perron equation (see, e.g., Ref. [67]),

$$\rho(x) = \int \rho(y)\delta(x - F(y))dy, \tag{37}$$

where $F(y) = 1 + m/y$ [see Eq. (29)[from which we get

$$\rho(x) = \rho\left(\frac{m}{x-1}\right)\frac{|m|}{(x-1)^2}. \tag{38}$$

For $m < -1/4$, a solution is given by the Lorentzian function

$$\rho(x) = \frac{1}{\pi}\frac{\gamma}{\left(x - \frac{1}{2}\right)^2 + \gamma^2}, \tag{39}$$

with $\gamma = \sqrt{|4m + 1|}/2$. Using this distribution, we get

$$\langle \ln |R_i| \rangle = \int \rho(x) \ln |x| dx = \frac{1}{2} \ln |m| \tag{40}$$

for $m < -1/4$, and

$$\langle \ln |R_i| \rangle = \ln |\bar{R}| = \ln \left|(1 + \sqrt{1 + 4m})/2\right| \tag{41}$$

for $m > -1/4$. It is easy to see that, from Eq. (34), there are two MZMs per edge if $m \in (-1, 0)$, and, from Eq. (33), there is one MZM per edge if $m \in (-1, 2)$, in agreement with Ref. [14].

B. Uncorrelated disorder

Let us now consider uncorrelated random variables m_i. For simplicity, we will consider a bimodal disorder, so m_i can be equal to $m_+ = m + \epsilon$ and $m_- = m - \epsilon$, with the same probability. As shown in Ref. [68], the distribution $\rho(R_i)$ is the solution of

$$\rho(x) = \frac{1}{2}\int \rho(y)[\delta(x - F(y; m_+)) + \delta(x - F(y; m_-))]dy, \tag{42}$$

where $F(y; m_\pm)$ is the map $F(x)$ with $m_i = m_\pm$, from which we get the equation

$$\rho(x) = \frac{1}{2}\rho\left(\frac{m_+}{x-1}\right)\frac{|m_+|}{(x-1)^2} + \frac{1}{2}\rho\left(\frac{m_-}{x-1}\right)\frac{|m_-|}{(x-1)^2}. \tag{43}$$

We look for a nontrivial solution of this equation. For $m < -1/4$, we get

$$\rho(x) = \frac{1}{\pi}\frac{\gamma}{\left(x-\frac{1}{2}\right)^2+\gamma^2} + \eta(x), \tag{44}$$

where $\gamma = \sqrt{|4m+1|}/2$, and $\eta(x) \sim \epsilon^2$ since Eq. (43) is satisfied for $\eta(x) = 0$ up to terms of the order ϵ^2. In particular, $\eta(x)$ is solution of

$$\eta(x) = g(x) + \eta\left(\frac{m}{x-1}\right)\frac{|m|}{(x-1)^2}, \tag{45}$$

where

$$g(x) = -\frac{\sqrt{|1+4m|}(m^2+3m(x-1)^2-(x-1)^3)}{2\pi m^2(m+x-x^2)^3}\epsilon^2 + O(\epsilon^3). \tag{46}$$

Since we are interested only on the mean value $\langle \ln|R_i|\rangle$, we can use the following equations:

$$\int \eta(x)\ln|x|dx = -\int \big(\eta(x)-g(x)\big)\ln|x-1|dx,$$

$$\int \eta(x)\ln|x|dx = \frac{1}{2}\int \big(\eta(x)\ln|x+m|dx + g(x)\ln|x|\big)dx,$$

which can be easily combined for $m = -1$, getting

$$\int \eta(x)\ln|x|dx = -\frac{\epsilon^2}{12} + O(\epsilon^3). \tag{47}$$

The effect of the disorder on widening or shrinking the boundary of the topological phase can be understood by considering the critical points in the absence of disorder. For the topological phase with two MZMs, we have the boundaries at $m = -1$ and $m = 0$ in the absence of disorder.

For $m = -1$, we get

$$\langle \ln|R_i|\rangle = -\frac{\epsilon^2}{12} + O(\epsilon^3). \tag{48}$$

On the other hand, at $m = 0$, we have that

$$\rho(x) = \tfrac{1}{4}(\delta(x-R_+)+\delta(x-R_-)+\delta(x-R'_+) + \delta(x-R'_-)) + O(\epsilon^3)$$

is the solution of Eq. (43), with $R_\pm = 1 \pm \epsilon - \epsilon^2 + O(\epsilon^3)$, $R'_\pm = 1 \pm \epsilon + \epsilon^2 + O(\epsilon^3)$. As a result, we get $\langle \ln|R_i|\rangle = \frac{1}{4}(\ln|R_+| + \ln|R_-| + \ln|R'_+| + \ln|R'_-|)$.

For $m = 0$ we have, therefore,

$$\langle \ln|R_i|\rangle = -\frac{\epsilon^2}{2} + O(\epsilon^3). \tag{49}$$

On both boundaries $m = -1$ and $m = 0$, we have $\langle \ln|R_i|\rangle < 0$, and since also $\langle \ln|m_i|\rangle$ is negative, from Eq. (34) we find that the topological region with two MZMs widens on both sides, switching on a small disorder ϵ.

On the other hand, for the topological phase with one MZM, we have the boundaries at $m = -1$ and $m = 2$ in the absence of disorder. At the point $m = -1$, we get

$$\langle \ln|m_i|\rangle = -\frac{\epsilon^2}{2} + O(\epsilon^3). \tag{50}$$

At $m = 2$, we get that, for small ϵ, $\rho(R_i)$ is uniform and equal to $1/(2\epsilon)$ for $R_i \in (2-\epsilon, 2+\epsilon)$ and zero otherwise, so

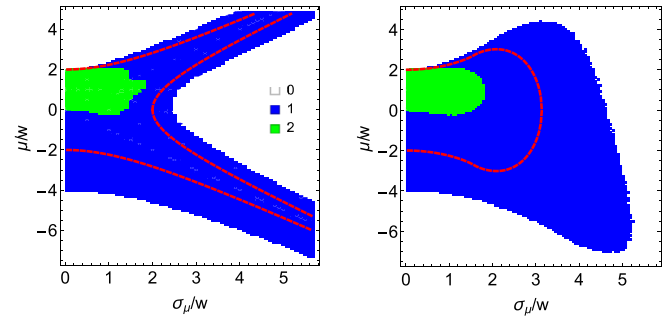

FIG. 2. Topological phase diagrams σ_μ-μ, for next-nearest-neighbor couplings, $r = 2$, and $w_1 = w_2 = \Delta_1 = \Delta_2$, obtained using the condition reported in Eqs. (33) and (34), averaging over $n = 10^5$ random variables. The diagrams are characterized by zero (white regions), one (blue regions), and two (green regions) MZMs per edge for two different distributions of the disorder: bimodal (left) and uniform box (right) distributions. For a better comparison with Fig. 1, the topological boundaries for $r = 1$ are reported by red dashed lines.

$\langle \ln|R_i|\rangle \simeq \ln(2) - \epsilon^2/24$. Moreover, close to $m = 2$, for small ϵ, from Eq. (18) we get $\langle \ln|m_i|\rangle \simeq \ln(2) - \epsilon^2/8$, so

$$\langle \ln|m_i|\rangle - \langle \ln|R_i|\rangle = -\frac{\epsilon^2}{8} + \frac{\epsilon^2}{24} + O(\epsilon^3). \tag{51}$$

From Eq. (33), we find that also the topological region with one MZM widens for small ϵ. We expect this behavior occurs also for other distributions of the disorder, namely, that the disorder increases the topological phase, since only the variance σ_m^2 of the random variables appears at the leading order.

Let us consider the case of large disorder. There are two different behaviors for the case of a continuous or discrete distribution. For the bimodal distribution, as shown in the left panel of Fig. 2, the topological region with one MZM per edge survives for large disorder strength, near the resonances $m \approx \pm\epsilon$. This behavior can be explained by noticing that $\langle \ln|m_i|\rangle = 1/2(\ln|m+\epsilon| + \ln|m-\epsilon|) \to -\infty$ for $m \to \pm\epsilon$, so the condition $\langle \ln|m_i|\rangle < 0$ for having one MZM is always satisfied. This behavior still exists for any discrete distribution of disorder with a finite number of values, while it disappears when the values of the distribution become dense in a certain interval, since in this case $\langle \ln|m_i|\rangle$ cannot diverge and becomes positive for large disorder. For a box distribution, for instance, where m_i are uniformly distributed in the interval $[m-\epsilon, m+\epsilon]$, the topological region is limited, as shown in the right panel of Fig. 2. In any case, upon increasing the range of the couplings, we observe an increase of the whole topological phase, as well as the appearance of an additional phase characterized by two MZMs per edge. In Fig. 2, in the topological phase diagram for $r = 2$, also the boundaries for the case $r = 1$ are reported (red dashed lines). Finally, we observe that for the case $w_\ell \neq \Delta_\ell$, we get essentially the same behavior. The only effect of having a larger or smaller paring with respect to the hopping parameter is that the topological phase can be increased or suppressed mainly in the disorder strength direction as shown in Fig. 3. In this latter case, we determine the number of MZMs by counting the number $v^<$ ($v^>$) of eigenvalues λ_n of $\tilde{\mathcal{A}}_n$ such that $|\lambda_n| < 1$ ($|\lambda_n| > 1$), as explained in Sec. II A.

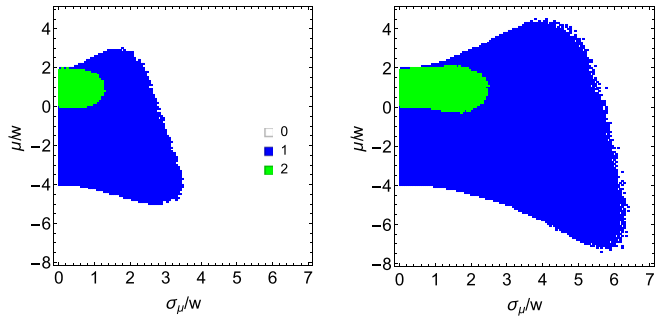

FIG. 3. Topological phase diagrams σ_μ-μ, for next-nearest-neighbor couplings, $r = 2$, and for parameters $w = w_1 = w_2$ and $\Delta = \Delta_1 = \Delta_2$ but $\Delta \neq w$. We consider a uniform disorder distribution and we average over 100 disorder configurations for a chain with $L = 200$ sites. In the left panel, $\Delta = w/2$, while in the right panel, $\Delta = 2w$.

C. Correlated disorder

Let us now investigate the effects of a correlated disorder, namely, when $\langle m_i m_j \rangle \neq \langle m_i \rangle \langle m_j \rangle$ for some i and j. A way to introduce a correlation in the disorder is the following. Let us consider

$$m_i = m + \epsilon x_i. \tag{52}$$

The random variables x_i can be chosen conveniently, in turn, written in terms of two other random variables y_i and z_i, to design two kinds of disorder:

(1) uncorrelated disorder, such that $x_i = (y_i + z_i)/2$ and

(2) correlated disorder, such that $x_{2i-1} = (y_{2i-1} + z_{2i-1})/2$ and $x_{2i} = s\,(y_{2i-1} + y_{2i})/2$, where $s = \pm 1$,

where z_i and y_i are uncorrelated random variables which take values -1 or 1 with equal probability. For both kinds of disorder, locally, at any site i, we get the same distribution $p(m_i) = \frac{1}{2} p_{bi}(m_i) + \frac{1}{2}\delta(m_i - m)$, where $p_{bi}(m_i) = \frac{1}{2}\delta(m_i - m - \epsilon) + \frac{1}{2}\delta(m_i - m + \epsilon)$ is the bimodal one. As a result, $\langle \ln |m_i| \rangle = 1/2 \ln |m| + (\ln |m + \epsilon| + \ln |m - \epsilon|)/4 < 0$, i.e., the first condition in Eqs. (33) and (34), is the same for both kinds of disorder. In contrast, the second condition in Eq. (33) for one MZM, $\langle \ln |m_i| \rangle < \langle \ln |R_i| \rangle$, and the second condition in Eq. (34) for two MZMs, $\langle \ln |R_i| \rangle < 0$, can be different for the two kinds of disorder. As shown in Figs. 4 and 5, correlations and anticorrelations have opposite effects.

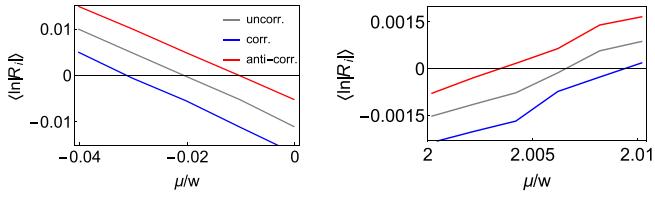

FIG. 4. $\langle \ln |R_i| \rangle$ as a function of the mean value of the chemical potential μ for uncorrelated, correlated ($s = +1$), and anticorrelated ($s = -$) disorder, averaging over $n = 10^6$ random variables, for $\epsilon = 0.2$ (where $\sigma_\mu/w = 2\epsilon$). In the interval under consideration, $\langle \ln |m_i| \rangle < 0$ is verified, so we get a topological phase with two MZMs per edge for $\langle \ln |R_i| \rangle < 0$.

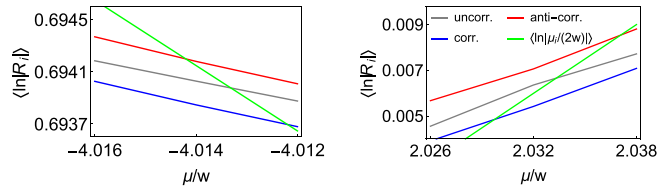

FIG. 5. $\langle \ln |R_i| \rangle$ as a function of μ, for uncorrelated, correlated ($s = +1$) and anticorrelated ($\sigma = -1$) disorder, with $\epsilon = 0.2$. The green line shows $\langle \ln |m_i| \rangle$ as a function of μ. We get a topological phase with one MZM per edge for $\langle \ln |R_i| \rangle > \langle \ln |m_i| \rangle$.

In detail, for two MZMs, the presence of correlated disorder ($s = +1$) widens the topological phase, while the presence of anticorrelation ($s = -1$) shrinks it (see Fig. 4). On the contrary, for one MZM, the presence of correlation ($s = +1$) shrinks the topological phase, while anticorrelation ($s = -1$) widens it (see Fig. 5).

D. Power-law coupling

We conclude our investigation for the case $r = 2$ by considering a power-law decay of the coupling parameters, $w_\ell = \Delta_\ell = w/\ell^\alpha$. In this case, the transfer matrix reads

$$A_i = \begin{pmatrix} -2^\alpha & 2^\alpha m_i \\ 1 & 0 \end{pmatrix}. \tag{53}$$

In this case, for $n \to \infty$, the determinant in Eq. (26) becomes

$$|\det(\tilde{A}_n)| \simeq 2^{n\alpha} e^{n\langle \ln |m_i| \rangle}, \tag{54}$$

while the trace in Eq. (27) is modified as follows:

$$|\mathrm{Tr}(\tilde{A}_n)| \simeq 2^{n\alpha} e^{n\langle \ln |R_i^\alpha| \rangle}, \tag{55}$$

where we define

$$R_i^\alpha = 1 + \frac{m_i}{2^\alpha R_{i-1}^\alpha}, \tag{56}$$

with $R_1^\alpha = 1$, so $R_i^0 = R_i$. This can be understood by noting that $\mathrm{Tr}(\tilde{A}_n)$ for $\alpha > 0$ is obtained from $\mathrm{Tr}(\tilde{A}_n)$, with $\alpha = 0$, by multiplying it by $2^{n\alpha}$ and by replacing m_i with $m_i/2^\alpha$. The condition Eq. (34) for two MZMs, then, is modified as follows:

$$\left\langle \ln \left| R_i^\alpha \right| \right\rangle < -\alpha \ln 2 \quad \text{and} \quad \langle \ln |m_i| \rangle < -\alpha \ln 2 \Rightarrow \exists\, 2 \text{ MZMs}. \tag{57}$$

We expect that $\langle \ln |R_i^\alpha| \rangle \geqslant -\ln 2$, where the equality holds for $m_i = -2^\alpha/4$, so the condition $\langle \ln |R_i^\alpha| \rangle < -\alpha \ln 2$ can be satisfied only if $\alpha < 1$. For the homogeneous case, $m_i = m$, it is easy to see that the inequality $\langle \ln |R_i^\alpha| \rangle \geqslant -\ln 2$ is satisfied. Furthermore, if $|m_i| \leqslant 2^\alpha/4$, the convergents are $R_i^\alpha \geqslant 1/2$ (see, e.g., Ref. [69]), therefore, also in this case $\langle \ln |R_i^\alpha| \rangle \geqslant -\ln 2$. As a result, we expect that, from Eq. (57), we can have two MZMs per edge only for $\alpha < 1$.

On the other hand, concerning the topological phase with one MZM, Eq. (33) is modified, getting the following condition:

$$\langle \ln |m_i| \rangle < -\alpha \ln 2 \quad \text{or} \quad \langle \ln |m_i| \rangle < \left\langle \ln \left| R_i^\alpha \right| \right\rangle \Rightarrow \exists\, 1 \text{ MZM}. \tag{58}$$

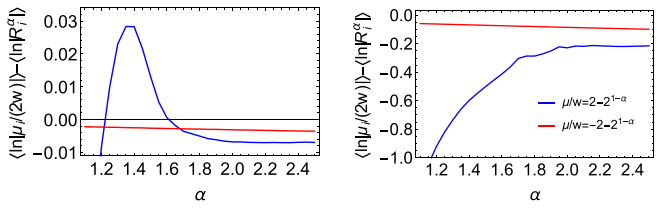

FIG. 6. $\langle \ln |m_i| \rangle - \langle \ln |R_i^\alpha| \rangle$, calculated for $n = 10^6$, as a function of $\alpha > 1$, for a bimodal distributed disorder with strength $\epsilon = 0.1$ in the left panel and $\epsilon = 0.5$ in the right panel. The topological phase with one MZM per edge is for negative values, $\langle \ln |m_i| \rangle - \langle \ln |R_i| \rangle < 0$.

Let us discuss the effects of a small disorder on the topological phases in this case.

For $\alpha > 1$, instead, we can have zero or one MZM per edge and we can consider only Eq. (58). In the absence of disorder, namely, for $m_i = m$, we get $\alpha \ln 2 + \langle \ln |m_i| \rangle > 0$, and from the condition $\langle \ln |m_i| \rangle - \langle \ln |R_i^\alpha| \rangle < 0$ we obtain that there is one MZM for $(2^{-\alpha} - 1) < m < (2^{-\alpha} + 1)$. For simplicity, let us consider a bimodal distribution, i.e., $m_i = m + \epsilon$ and $m_i = m - \epsilon$ with the same probability and focus on the points $m = \pm 1 + 2^{-\alpha}$. As shown in Fig. 6, we get that the topological phase with one MZM can be suppressed, only at the boundary $m \approx -1 + 2^{-\alpha}$ (i.e., at $\mu/w \approx 2 - 2^{1-\alpha}$) for ϵ small enough, while it widens otherwise.

For $\alpha < 1$, we can have zero, one, or two MZMs. In the absence of disorder, i.e., for $m_i = m$, there is one MZM for $-2^{-\alpha} < m < (1 + 2^{-\alpha})$ and two MZMs if $-2^{-\alpha} < m < (2^{-\alpha} - 1)$. Let us focus on the phase with one MZM in the presence of disorder, defined by the condition given in Eq. (58). For small ϵ, $\langle \ln |m_i| \rangle - \langle \ln |R_i| \rangle$ is negative at both boundaries, $m = -2^{-\alpha}$ and $m = 1 + 2^{-\alpha}$, which means that the topological phase widens (see Fig. 7). On the contrary, concerning the phase with two MZMs, defined by the condition in Eq. (57), for small ϵ, $\alpha \ln 2 + \langle \ln |m_i| \rangle < 0$ at both boundaries $m = -2^{-\alpha}$ and $m = 2^{-\alpha} - 1$, while $\alpha \ln 2 + \langle \ln |R_i| \rangle$ is positive only for large α, so in this case the topological phase shrinks (see Fig. 7).

V. MANY-NEIGHBOR COUPLINGS ($r > 2$)

Similarly to what we have done for $r = 2$, let us consider, for simplicity, $\Delta_\ell = w_\ell$, starting first with the extreme case

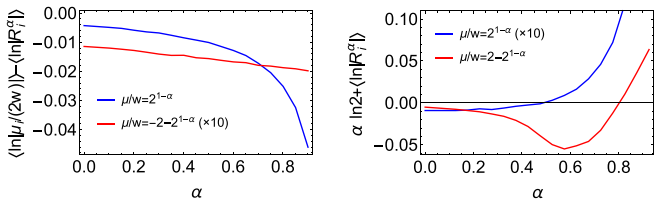

FIG. 7. $\langle \ln |m_i| \rangle - \langle \ln |R_i^\alpha| \rangle$ (left panel) and $\alpha \ln 2 + \langle \ln |R_i^\alpha| \rangle$ (right panel) calculated for $n = 10^6$, as functions of $\alpha < 1$, for a bimodal distributed disorder with strength $\epsilon = 0.1$. The topological phase with one MZM per edge is defined for $\langle \ln |m_i| \rangle - \langle \ln |R_i^\alpha| \rangle < 0$ while the phase with two MZMs for $\alpha \ln 2 + \langle \ln |R_i^\alpha| \rangle < 0$.

where $w_\ell = 0$ for any $\ell < r$ but $w_r \neq 0$. From Eq. (4), we get

$$\phi_{i+r} + \frac{\mu_i}{2w_r}\phi_i = 0, \tag{59}$$

from which we obtain r equations for $i_0 = 1, 2, \ldots, r$,

$$\phi_{rn+i_0} = \prod_{i=0}^{n-1} \left(-\frac{\mu_{ri+i_0}}{2w_r} \right) \phi_{i_0}, \tag{60}$$

which generalizes Eqs. (14) and (21). We now have r copies of the condition for getting one MZM,

$$\left\langle \ln \left| \frac{\mu_i}{2w_r} \right| \right\rangle_{i_0} < 0, \tag{61}$$

where we define the averages $\langle x_i \rangle_{i_0} = r/n \sum_i x_{ri+i_0}$, valid for large n. In detail, $i = 1, \cdots, r$ so we have r conditions. If locally the distribution probability of the disorder is the same at any site, the r conditions in Eq. (61) (with $i_0 = 1, \ldots, r$) are equal, and we can get only zero or r MZMs per edge. For general couplings, instead, we can have an intermediate number of MZMs.

Let us now consider nonvanishing w_ℓ focusing our attention, for simplicity, always to the case $w_\ell = \Delta_\ell$.

For $r = 3$, for instance, to determinate the eigenvalues λ_n of $\tilde{A}_n$, we have to solve the following equation:

$$\lambda_n^3 - \lambda_n^2 T_n + \lambda_n T_n' - D_n = 0, \tag{62}$$

where, to simplify notation, we define $T_n = \mathrm{Tr}(\tilde{A}_n)$, $T_n' = ((\mathrm{Tr}(\tilde{A}_n))^2 - \mathrm{Tr}(\tilde{A}_n^2))/2$ and $D_n = \det(\tilde{A}_n)$. From Eq. (62), we derive the following conditions:

$$D_n \to 0 \ \text{ and } \ T_n' \to 0 \ \text{ and } \ T_n \to 0 \Rightarrow \exists\, 3 \text{ MZMs}, \tag{63}$$

$$(D_n \to 0 \ \text{ and } \ T_n' \to 0) \text{ or } \left(\frac{D_n}{T_n} \to 0 \ \text{ and } \ \frac{T_n'}{T_n} \to 0 \right) \Rightarrow \exists\, 2 \text{ MZMs}, \tag{64}$$

$$D_n \to 0 \ \text{ or } \ \frac{D_n}{T_n} \to 0 \ \text{ or } \ \frac{D_n}{T_n'} \to 0 \ \Rightarrow \exists\, 1 \text{ MZM}. \tag{65}$$

As discussed in Appendix B, we expect that these conditions can be also expressed in terms of random continued fractions analogously to the next-nearest-neighbor case.

Equations (63)–(65) can be generalized for an arbitrary r, as shown in Appendix C. In particular, we note that the condition in Eq. (63) can be easily generalized to

$$\det(\tilde{A}_n) \to 0 \ \text{ and } \ \mathrm{Tr}\left(\tilde{A}_n^k\right) \to 0, \forall k \in I_{1,r-1} \Rightarrow \exists\, \mathrm{r} \text{ MZMs}, \tag{66}$$

where $I_{i,j} = \{i, i+1, \cdots, j\}$. Furthermore, for an arbitrary range r, $\det(\tilde{A}_n) \to 0$ is a sufficient (but not necessary) condition for getting one MZM per edge, and since $|\det(\tilde{A}_n)| \sim |w_1/w_r|^n e^{n\langle \ln |m_i| \rangle}$, we get that the condition $\langle \ln |m_i| \rangle < -\ln |w_1/w_r|$ implies that there is one MZM. As a result, if $|w_1| \geqslant |w_r|$, the topological phase with one MZM for $r > 1$ cannot be smaller than that for $r = 1$, for the same disorder and coupling w_1.

Finally, for $w_\ell = w$, without disorder there are zero, one, or r MZMs (see Ref. [14]). In detail, there are r MZMs if $m \in (-1, 0)$ and there is one MZM if $m \in (0, r)$. In the

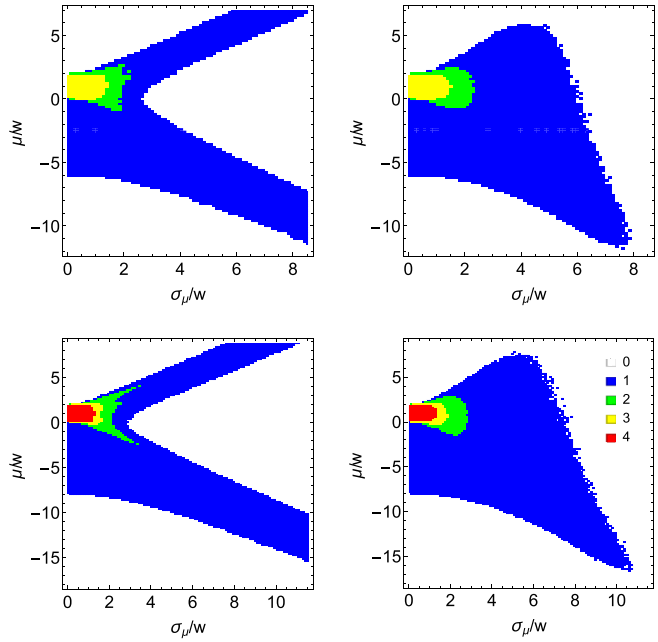

FIG. 8. Topological phase diagrams σ_μ-μ, for $r = 3$ (upper panels) and $r = 4$ (lower panels), for $w = w_1 = w_2 = \Delta_1 = \Delta_2$, with $L = 200$. The diagrams are characterized by zero (white), one (blue), two (green), three (yellow), and four (red) MZMs per edge, for a bimodal distribution (left panels) and a uniform disorder distribution (right panels).

presence of the disorder, instead, we can have many phases, with a number of MZMs which goes from 0 to r, as shown in Fig. 8. Moreover, we note that a large disorder significantly increases the topological regions.

VI. INFINITE NUMBER OF NEIGHBORS

To investigate the limit $r \to \infty$ corresponding to an infinite number of neighbors, we consider the following algebraically decaying parameters $w_\ell = w/\ell^\alpha$ and $\Delta_\ell = \Delta/\ell^\beta$. In the absence of disorder, namely, for a homogeneous chemical potential $\mu_i = \mu$, and for α and β greater than 1, in the thermodynamic limit, we can have zero or one MZMs per edge, if the Majorana number $\mathcal{M} = \mathrm{sgn}((\mu + g(0)w)(\mu + g(\pi)w))$ is 1 or -1, where $g(k) = 2\mathrm{Re}[Li_\alpha(e^{ik})]$, with $Li_\alpha(x)$ the polylogarithm. In the presence of disorder, we expect also that, for exponents larger than one, there are zero or one MZMs per edge, as for finite r.

We consider an uncorrelated box distribution, namely where the random variables are uniformly distributed, $m_i = m + \epsilon x_i$ with x_i uniform in $[-1, 1]$. For an open chain, described by the Hamiltonian $H = \frac{1}{4}\sum_{l,m} c_l \mathcal{H}_{lm} c_m$, as that in Eq. (2), we can calculate the following topological invariant:

$$W = \mathrm{Sig}(X\Gamma + \mathcal{H}), \tag{67}$$

as defined in Ref. [70]. Specifically, the signature $\mathrm{Sig}(M)$ of a matrix M is defined as the number of positive eigenvalues of M minus the number of negative ones. We define the position operator $X = \mathrm{diag}(X_j) \otimes I_2$, where the positions X_j are normalized such that $-1/2 \leqslant X_j \leqslant 1/2$, and the grading operator $\Gamma = I_L \otimes \tau_3$, where τ_i with $i = 1, 2, 3$ are the Pauli matrices and I_n the $n \times n$ identity matrix.

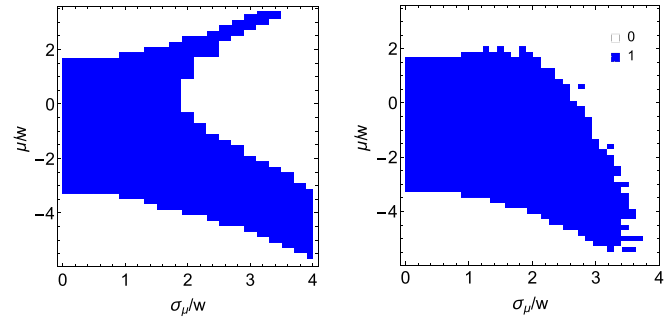

FIG. 9. Topological phase diagram σ_μ-μ for long-range couplings $w_\ell = \Delta_\ell = w/\ell^\alpha$ with $\alpha = 2$, obtained considering a chain with size $L = 200$ and averaging over 100 disorder realizations, with bimodal distribution (left), with $m_i = m \pm \epsilon$, namely, $\mu_i = \mu \pm \sigma_\mu$, and uniform box distribution (right), $m_i \in [m - \epsilon, m + \epsilon]$, namely, $\mu_i \in [\mu - \sqrt{3}\sigma_\mu, \mu + \sqrt{3}\sigma_\mu]$, characterized by zero (white region) and one (blue region) MZM.

We find that either a discrete bimodal distribution and a uniformly distribution of the disorder, on a chain with long range coupling $w_\ell = \Delta_\ell = w/\ell^\alpha$, for $\alpha > 1$, induce qualitatively similar behaviors as those found for a finite number of neighbors, supporting and widening the topological phases, see Fig. 9. As shown in the two panels of Fig. 9, for both distributions, the topological phases are not symmetric, as for the cases with finite $r > 1$, for relatively small α. They become symmetric around $\mu = 0$ for $\alpha \gg 1$, recovering the short-range results reported in Fig. 1.

Let us now discuss in more detail the small disorder regime. As shown in Fig. 10, where W is reported varying μ, always for $w_\ell = \Delta_\ell$ and for very small disorder, the topological phase widens for $\mu \approx -g(\pi)w > 0$ (top panel) and slightly shrinks for $\mu \approx -g(0)w < 0$ (bottom panel) for α not too large. However, since the limit $\alpha \to \infty$ is equivalent to the case $r = 1$, we expect that, for α large enough, the topological region widens again at both boundaries.

In general, this behavior can be explained by considering the effective Hamiltonian

$$H_e = H_0 + \Sigma, \tag{68}$$

where Σ is the self-energy defined such that

$$\langle G \rangle = G_e, \tag{69}$$

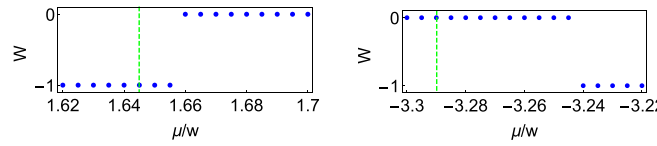

FIG. 10. Topological invariant W, Eq. (67), as a function of μ, for $L = 200$, and $w_\ell = \Delta_\ell = w/\ell^\alpha$ with $\alpha = 2$ at fixed small disorder $\epsilon = 0.2$ (fixed $\sigma_\mu/w = 2\epsilon/\sqrt{3}$), close to the two boundaries for a clean system. $W = 0$ corresponds to a trivial phase, $W = -1$ to a topological phase. The green dashed lines correspond to the critical values in the absence of disorder.

where we have defined the Green's functions $G = (E - H)^{-1}$ and $G_e = (E - H_e)^{-1}$, and where the average is done over disorder. H_0 is the clean Hamiltonian as in Eq. (2) with homogeneous $\mu_i = \mu$, so $H = H_0 + H_1$, where H_1 is the disorder term such that $\langle H_1 \rangle = 0$. To determinate the self-energy, we define $H_1' = H_1 - \Sigma$, then the Green's function reads

$$G = \frac{1}{E - H_e - H_1'}, \tag{70}$$

and by considering H_1' as a small perturbation, we get at second order

$$G \approx G_e(1 + H_1' G_e + H_1' G_e H_1' G_e). \tag{71}$$

By taking the average of this equation, we get

$$\langle H_1' \rangle + \langle H_1' G_e H_1' \rangle \approx 0, \tag{72}$$

and since $\langle H_1' \rangle = -\Sigma$ we have

$$\Sigma \approx \left\langle H_1' \frac{1}{E - H_0 - \Sigma} H_1' \right\rangle. \tag{73}$$

Since we are interested in small disorder, we consider Σ as a second-order correction, thus we get

$$\Sigma \approx \langle H_1 G_0 H_1 \rangle, \tag{74}$$

where $G_0 = (E - H_0)^{-1}$. For our model, the self-energy Σ, at $E = 0$ in the bulk, reads (see Appendix D)

$$\Sigma \approx -\frac{i}{2} \sum_j \delta\mu \, c_{2j-1} c_{2j} + \frac{i}{2} \sum_{\ell,j} [(\delta w_\ell + \delta\Delta_\ell) c_{2j} c_{2j+2\ell-1} - (\delta w_\ell - \delta\Delta_\ell) c_{2j-1} c_{2j+2\ell}]. \tag{75}$$

Adding Σ to H_0, we obtain the effective Hamiltonian H_e whose parameters are an effective chemical potential, $\mu + \delta\mu$, where

$$\delta\mu = -\frac{\sigma_\mu^2}{\pi} \int_0^\pi dk \frac{\mu + w g(k)}{(\mu + w g(k))^2 + (\Delta f(k))^2}, \tag{76}$$

an effective long-range hopping, $w_\ell + \delta w_\ell$, where

$$\delta w_\ell = -\frac{\sigma_\mu^2}{\pi} \int_0^\pi dk \cos(k\ell) \frac{\mu + w g(k)}{(\mu + w g(k))^2 + (\Delta f(k))^2}, \tag{77}$$

and an effective pairing, $\Delta_\ell + \delta\Delta_\ell$, where

$$\delta\Delta_\ell = -\frac{\sigma_\mu^2}{\pi} \int_0^\pi dk \sin(k\ell) \frac{\mu + w g(k)}{(\mu + w g(k))^2 + (\Delta f(k))^2}, \tag{78}$$

where μ and σ_μ^2 are the mean value and the variance of the disorder in the chemical potential, $g(k) = 2\mathrm{Re}[Li_\alpha(e^{ik})]$ and $f(k) = 2\mathrm{Im}[Li_\beta(e^{ik})]$. To characterize the topological phases, we can use the Majorana number of the effective Hamiltonian H_e.

Let us consider $w_\ell = \Delta_\ell$. For $\mu = -w g(0) < 0$, we get $\delta\mu > 0$, and $\delta w_\ell \approx -c' \delta\mu \ell^{-\alpha'}$ where α' increases with α, and where $c' > 0$. We can, then, calculate the Majorana number

$$\mathcal{M} \approx \mathrm{sgn}[(\delta\mu - c' \delta\mu g'(0))(w g(\pi) - w g(0))], \tag{79}$$

where $g'(k) = \sum_\ell \cos(k\ell) \ell^{-\alpha'} = 2\mathrm{Re}[Li_{\alpha'}(e^{ik})]$. We have that $w g(\pi) - w g(0) < 0$ and $1 - c' g'(0) < 0$ for any α', if $c' > 1/2$, or for α' not too large, if $c' < 1/2$. We find that c' is small, so $\mathcal{M} > 0$ (trivial phase) for α not too large. On the other hand, for $\mu = -w g(\pi) > 0$, we get $\delta\mu < 0$, and $\delta w_\ell \approx c'' \delta\mu (-1)^\ell \ell^{-\alpha''}$ where $c'' > 0$. Then, we get

$$\mathcal{M} \approx \mathrm{sgn}[(\delta\mu + c'' \delta\mu g''(\pi))(w g(0) - w g(\pi))], \tag{80}$$

where $g''(k) = \sum_\ell \cos(k\ell)(-1)^\ell \ell^{-\alpha''}$. We have that $g''(\pi) > 0$ for any α'', so $\mathcal{M} < 0$ (topological phase) for any α.

In the end, we note that for $w_l \neq \Delta_l$ and $w_l = \Delta_l$ the MZMs wave functions remain algebraically and exponentially localized, respectively, also in the presence of disorder (see Fig. 11). This can be explained by using the method of Ref. [65]. By considering the self-energy for small disorder, we get the wave function of a MZM,

$$\phi_j \sim \mathrm{Im} \oint_{|z|=1} \frac{z^{j-1} dz}{\mu + \delta\mu + w\tilde{g}(z) + \Delta\tilde{f}(z) + Y(z)}, \tag{81}$$

where $\tilde{g}(z) = (Li_\alpha(z) + Li_\alpha(1/z))$, $\tilde{f}(z) = (Li_\beta(z) - Li_\beta(1/z))$ and where $Y(z)$ is defined by performing an analytical continuation in the complex plane such that

$$Y(e^{ik}) = \sum_\ell (\delta w_\ell \cos(k\ell) + i\delta\Delta_\ell \sin(k\ell)). \tag{82}$$

$Y(z)$ has no branch cut for $|z| < 1$. Then, for $\Delta_\ell \neq w_\ell$ we get a branch cut coming from the polylogarithms. As a result, we get an algebraically decay of the wave function, while for $\Delta_\ell = w_\ell$ there is no branch cut and we get a purely exponential decay, as in the absence of disorder [65,66]. We note that since the corrections δw_ℓ and $\delta\Delta_\ell$, and therefore the effective couplings, are different, also for $\Delta_\ell = w_\ell$, one might expect that the MZMs become algebraically localized in the presence of disorder. However, this case does not occur

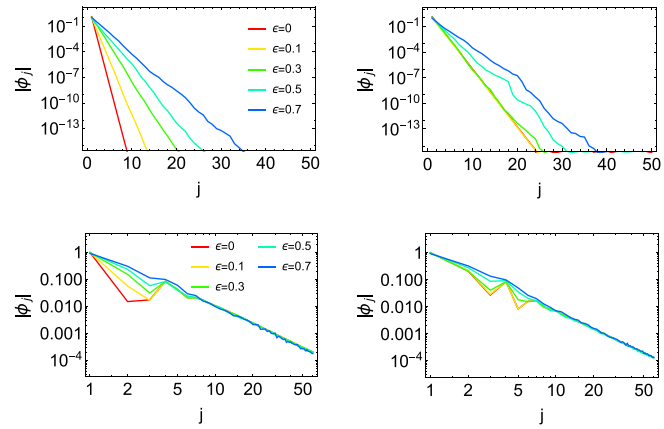

FIG. 11. Top: Wave function ϕ_j of a MZM, as a function of the distance j from the edge, for $L = 200$, $w_\ell = \Delta_\ell = w/\ell^\alpha$ with $\alpha = 2$, for different values of the disorder strength ϵ, at $\mu/(2w) = 0.01$ (left panel) and $\mu/(2w) = 0.2$ (right panel). We average over 100 disorder realizations. The plots are in linear-log scale, showing exponential decays. Bottom: Wave- unction ϕ_j of a MZM, as a function of the distance j from the edge, for $L = 200$, with $w_\ell \neq \Delta_\ell$, in particular, $w_\ell = w/\ell^\alpha$ and $\Delta = w/\ell^\beta$ with $\alpha = 4$ and $\beta = 2$. We consider different values of the disorder strength ϵ, at $\mu/(2w) = 0.01$ (left panel) and $\mu/(2w) = 0.2$ (right panel). The plots are in log-log scale, showing algebraic decays.

because of the analytic properties of the function $Y(z)$. In particular, for $\Delta_\ell = w_\ell$, the MZMs stay exponentially localized with a localization length which increases upon increasing the strength of the disorder (see Fig. 11, top panels). In the other case, for $\Delta_\ell \neq w_\ell$ the MZMs remain algebraically localized (see Fig. 11, bottom panels) as in the absence of disorder.

VII. CONCLUSIONS

We carried out a complete study of the combined effects related to the interplay of disorder and range of the couplings on the topological phase diagrams for a one-dimensional topological superconductor. We considered both a finite and infinite number of neighbors involved in the couplings.

Our work is in perfect agreement with what is known in the previous literature, namely, that disorder can stabilize the topological order (see, for instance, Ref. [63] for one-dimensional models and Ref. [45] for the multichannel models). In particular, we generalize what has been found in Ref. [24] for a one-dimensional topological superconductor described by a short-range Kitaev chain in the presence of disorder by considering longer finite-range and infinite-range couplings, with two different kinds of random distributions. We show that both the coupling range and the disorder can promote the topological order.

For finite-range couplings, we resorted to a transfer matrix approach which allowed us to derive the conditions for the existence of MZMs, and to show that either the range or the on-site disorder can greatly enhance the topological phases characterized by the appearance of one or many Majorana modes localized at the edges. Moreover, we discussed the role of correlated disorder which can further widen the topological regions. We always performed a comparing analysis considering a discrete and a continuous disorder distribution. In the former case, the topological regions extend to regimes of infinitely strong disorder. Finally, we show that, for long-range couplings, the spatial decay of the edge modes remains algebraic or exponential for equal hopping and pairing, even in the presence of disorder.

In conclusion, our results show that the combined effects of disorder and range of the couplings can generate nontrivial behaviors, increasing the number of phases and greatly widening their extension.

ACKNOWLEDGMENTS

The authors acknowledge financial support from Project BIRD 2021, "Correlations, dynamics and topology in long-range quantum systems" of the Department of Physics and Astronomy, University of Padova, and and from the European Union-Next Generation EU within the National Center for HPC, Big Data and Quantum Computing (Project No. CN00000013, CN1 Spoke 10—Quantum Computing).

APPENDIX A: TRACE OF $\tilde{A}_n$ for $r = 2$

Let us calculate $\tilde{A}_n$ for $r = 2$ considering the case with $\Delta_\ell = w_\ell$, with $w_1 = w_2$, and n even. By using the multiplication law,

$$A_2 A_1 = \mathrm{diag}(m_2, m_1) - A_1, \tag{A1}$$

[which, however, can be easily generalized for $w_1 \neq w_2$ to $A_2 A_1 = \mathrm{diag}(m_2, m_1) - t_1 A_1$, with $m_i = -\mu_i/(2w_2)$ and $t_1 = -w_1/w_2$], where $\mathrm{diag}(m_2, m_1)$ is the diagonal matrix with elements m_2 and m_1, we get

$$\tilde{A}_n = d_{n,1} - A_n\, d_{n-1,1} - A_{n-1}\, d_{n-2,1} - \cdots - A_3\, d_{2,1} - A_1, \tag{A2}$$

where we define $d_{2,1} = \mathrm{diag}(m_2, m_1)$, $d_{3,1} = \mathrm{diag}(m_3, m_1)$, $d_{4,1} = \mathrm{diag}(m_4, m_1) + \mathrm{diag}(m_4, m_3)\,\mathrm{diag}(m_2, m_1)$ and so on. In general terms, $d_{i,1}$ is the diagonal matrix obtained by summing all the products of the form $\mathrm{diag}(m_i, m_{i_k})\,\mathrm{diag}(m_{i_k-1}, m_{i_{k-1}}) \cdots \mathrm{diag}(m_{i_1-1}, m_1)$, where $i_j > i_{j-1} + 1$ and $i_1 > 2$. The trace is

$$\begin{aligned}\mathrm{Tr}(\tilde{A}_n) = \mathrm{Tr}(d_{n,1}) - \mathrm{Tr}(A_n d_{n-1,1}) - \mathrm{Tr}(A_{n-1} d_{n-2,1}) - \cdots \\ - \mathrm{Tr}(A_3 d_{2,1}) - \mathrm{Tr}(A_1).\end{aligned} \tag{A3}$$

Since $\mathrm{Tr}(A_i\,\mathrm{diag}(a, b)) = -a$, we get

$$\mathrm{Tr}(\tilde{A}_n) = \mathrm{Tr}(d_{n,1}) + d^1_{n-1,1} + d^1_{n-2,1} + \cdots + d^1_{2,1} + 1, \tag{A4}$$

where d^1 is the element (1,1) of the diagonal matrix d. In particular,

$$d^1_{i,1} = \sum_l p^u_i(l), \tag{A5}$$

where $p^u_i(l)$ are all the products of the upper endpoints of the noncrossing partitions of $(m_i, m_{i-1}, \cdots, m_1)$ with at least two elements, e.g., the noncrossing partitions of $(m_5, m_4, m_3, m_2, m_1)$ are $(m_5, m_4, m_3, m_2, m_1)$, $(m_5, m_4) \cup (m_3, m_2, m_1)$, and $(m_5, m_4, m_3) \cup (m_2, m_1)$, then $d^1_{5,1} = m_5 + m_5 m_3 + m_5 m_2$. We get the relation

$$d^1_{i,1} = m_i\big(1 + d^1_{i-2,1} + d^1_{i-3,1} + \cdots + d^1_{2,1}\big). \tag{A6}$$

By defining $p^\ell_i(l)$ as all the products of the lower endpoints, we get

$$d^2_{i,1} = \sum_l p^\ell_i(l). \tag{A7}$$

Since $\mathrm{Tr}(d_{i,1}) = d^1_{i,1} + d^2_{i,1}$, the trace of $\tilde{A}_n$ is then given by

$$\mathrm{Tr}(\tilde{A}_n) = 1 + \sum_{i=1}^{n} m_i + \sum_{j=4}^{n} \sum_{i=2}^{j-2} m_j m_i + m_1 \sum_{i=3}^{n-1} m_i + \cdots, \tag{A8}$$

where we omitted products with more than two terms. We can rewrite it as

$$\begin{aligned}\mathrm{Tr}(\tilde{A}_n) = 1 + \sum_{i=1}^{n} m_i + \frac{1}{2}\left(\sum_{i=2}^{n} m_i\right)^2 - \frac{1}{2}\sum_{i=2}^{n} m_i^2 \\ - \sum_{i=3}^{n} m_i m_{i-1} + m_1 \sum_{i=3}^{n-1} m_i + \cdots,\end{aligned} \tag{A9}$$

and, therefore, for large n, we can write Eq. (30). To evaluate the large n limit of the trace, we note that, if $m_n \neq 0$,

$$\mathrm{Tr}(\tilde{A}_{n-2}) = d^2_{n-2,1} + \frac{d^1_{n,1}}{m_n}, \tag{A10}$$

and $d^2_{n,1}$ can be obtained from $d^1_{n,1}$ by permuting the site indices as follows: $n \leftrightarrow 1$, $n-1 \leftrightarrow 2$, and so on. Thus, we

have to calculate the large-n limit of $d^1_{n,1}$. Actually, we have to determine when $\lim_{n\to\infty} d^1_{n,1} = 0$. We get

$$d^1_{i,1} = \frac{m_i}{m_{i-1}} R_{i-2} d^1_{i-1,1}, \tag{A11}$$

where we have defined

$$R_i = \frac{1 + \sum_{j=2}^{i} d^1_{j,1}}{1 + \sum_{j=2}^{i-1} d^1_{j,1}}, \tag{A12}$$

which fulfills Eq. (29), with $R_1 = 1$, and therefore, can be written as a random continued fraction, Eq. (28). Thus, we get $|\mathrm{Tr}(\tilde{A}_n)| \sim \prod_{i=1}^{n} |R_i| = e^{n\langle \ln |R_i| \rangle}$ as $n \to \infty$, where the average can be evaluated using the probability distribution of the convergents R_i.

An alternative way to derive the trace $\mathrm{Tr}(\tilde{A}_n)$ is the following. Performing the products, we get

$$\begin{aligned}\mathrm{Tr}(\tilde{A}_n) = (-1)^n \{ & m_2[m_4(m_6(\cdots)) \\ & + m_5(\cdots)] + m_3(m_5(\cdots)) + m_4(\cdots) \\ & + m_1[m_3(m_5(\cdots)) + m_4(\cdots)]\}. \end{aligned} \tag{A13}$$

This expression can be obtained rewriting A_i as

$$A_i = B - m_i C, \tag{A14}$$

where $B = \left(\begin{smallmatrix} -1 & 0 \\ 1 & 0 \end{smallmatrix}\right)$ and $C = \left(\begin{smallmatrix} 0 & -1 \\ 0 & 0 \end{smallmatrix}\right)$. The matrices C, B, CB, and BC form a closed algebra and are such that

$$BB = -B,\ CC = 0,\ BCB = -B,\ CBC = -C \tag{A15}$$

and

$$\mathrm{Tr}(B) = \mathrm{Tr}(CB) = \mathrm{Tr}(BC) = -1, \quad \mathrm{Tr}(C) = 0. \tag{A16}$$

Making the product $A_i A_{i-1}$, we get $B \to -B$ or $B \to -m_i CB$, and $CB \to -B$, while $C \to BC$ and $BC \to -BC$ or $BC \to m_i C$. We can draw two graphs which are two trees of descendants with ancestors B and C: the first generates only a cascade of B and CB while the latter generates BC and C. The trace is, therefore, equal to the sum of all possible paths along the tree graphs, excluding those which end with C, since $\mathrm{Tr}(C) = 0$. The number of these paths, after n steps, are $F_n + 2F_{n-1}$, where F_n are the Fibonacci numbers. From Eq. (A13) or by counting the paths as described above, we get that, after relabeling $i \leftrightarrow n - i$, we have to solve the following recursive equations:

$$\mathcal{F}_i = \mathcal{F}_{i-1} + m_i \mathcal{F}_{i-2}, \tag{A17}$$

with initial conditions $\mathcal{F}_0 = 0$ $\mathcal{F}_1 = 1$, such that, given the solution $\mathcal{F}_n$, the trace of $\tilde{A}_n$, for large n, is

$$\mathrm{Tr}(\tilde{A}_n) = (-1)^n (\mathcal{F}_n + 2m\,\mathcal{F}_{n-1}), \tag{A18}$$

which can be also written as $\mathrm{Tr}(\tilde{A}_n) = (-1)^n (2\,\mathcal{F}_{n+1} - \mathcal{F}_n)$. Notice that, for $m_i = 1$, from Eq. (A17), we get $\mathcal{F}_n = F_n$, the Fibonacci numbers, then $\mathrm{Tr}(\tilde{A}_n) = (-1)^n (F_n + 2F_{n-1})$. Generally, for integer $m_i = m$, the solution $\mathcal{F}_n$ of Eq. (A17) is a Lucas sequence, named the $(1, m)$-Fibonacci sequence.

Defining the ratio

$$R_i = \frac{\mathcal{F}_i}{\mathcal{F}_{i-1}}, \tag{A19}$$

Eq. (A17) can be written as $R_i = 1 + \frac{m_i}{R_{i-1}}$, which is Eq. (29). As a result, $|\mathrm{Tr}(\tilde{A}_n)| \simeq |\mathcal{F}_n| = \prod_{i=2}^{n} |R_i|$.

APPENDIX B: CASE $r = 3$

Let us investigate the case with $r = 3$, focusing on $\Delta_\ell = w_\ell = w$. It is easy to see that $D_n = \det(\tilde{A}_n) = \prod_{i=1}^{n} m_i$, therefore $|D_n| = e^{n\langle \ln |m_i| \rangle}$. To evaluate the trace $T_n = \mathrm{Tr}(\tilde{A}_n)$ and $T'_n = ((\mathrm{Tr}(\tilde{A}_n))^2 - \mathrm{Tr}(\tilde{A}_n^2))/2$, we consider n as a multiple of 3, i.e., $n = 3k$ with k a positive integer. For T_n, we get

$$T_n = 2 + \sum_{i_e} p_n(i_e), \tag{B1}$$

where $p_n(i_e)$ are all the different products (without repetitions) of the lower endpoints of the noncrossing partitions of $(m_n, m_{n-1}, \cdots, m_1)$ and cyclic permutations, e.g., $(m_{n-1}, \cdots, m_1, m_n)$ and so on, with $3k$ elements with k nonnegative integer, e.g., for $n = 6$, we get $T_6 = 2 + \sum_{i=1}^{6} m_i + m_1 m_4 + m_2 m_5 + m_3 m_6$, where m_i comes from the partition $(m_{i-1}, \cdots, m_1, m_6, \cdots, m_i)$, $m_1 m_4$ comes from the partition $(m_6, m_5, m_4) \cup (m_3, m_2, m_1)$, $m_2 m_5$ comes from the partition $(m_1, m_6, m_5) \cup (m_4, m_3, m_2)$, and $m_3 m_5$ comes from the partition $(m_2, m_1, m_6) \cup (m_5, m_4, m_3)$. Concerning T'_n, we get

$$T'_n = 1 + \sum_{i_e} p'_n(i_e), \tag{B2}$$

where $p'_n(i_e)$ are all the different products of the lower endpoints of certain noncrossing partitions of $(m_n, m_{n-1}, \cdots, m_1)$ and cyclic permutations, e.g., $(m_{n-1}, \cdots, m_1, m_n)$ and so on, e.g., for $n = 3$, we get $T'_3 = 1 + \sum_{i=1}^{3} m_i + m_1 m_2 + m_1 m_3 + m_2 m_3$.

We note that we can write T_n and T'_n in the forms $T_n = e^{n\langle \ln |K_l| \rangle}$ and $T'_n = e^{n\langle \ln |K'_l| \rangle}$, where K_l and K'_l are continued fractions uniquely determined by $(m_l, m_{l-1}, \cdots, m_1)$. Let us consider T_n. We define s_i with $i = 1, \cdots, n$ the solutions of the n equations

$$\begin{aligned} 2 + \sum_{i_e} p_l(i_e) = {} & s_1(s_1 + s_1 s_2) \cdots (s_1 + s_1 s_2 + \cdots \\ & + s_1 s_2 \cdots s_l) \end{aligned}$$

for $l = 1, \cdots, n$, with $p_l(i_e)$ as defined above. The terms $K_l \equiv (s_1 + s_1 s_2 + \cdots + s_1 s_2 \cdots s_l)$ can be written as Euler's continued fractions, therefore, we can write $|T_n| = \prod_{l=1}^{n} |K_l| = e^{n\langle \ln |K_l| \rangle}$. An analogous form can be obtained for T'_n.

APPENDIX C: ARBITRARY r

For an arbitrary r, for $w_\ell = \Delta_\ell$, we get the following generalized eigenvalue equation:

$$\sum_{k=0}^{r} (-1)^k \lambda_n^{r-k} T_n^{(k)} = 0, \tag{C1}$$

where $T_n^{(k)} = \mathrm{Tr}(\bigwedge^k \tilde{A}_n)$ is the trace of the kth exterior power of $\tilde{A}_n$, which is defined by

$$T_n^{(k)} = \frac{1}{k!} \det \begin{pmatrix} \mathrm{Tr}(\tilde{A}_n) & k-1 & 0 & \cdots & 0 \\ \mathrm{Tr}(\tilde{A}_n^2) & \mathrm{Tr}(\tilde{A}_n) & k-2 & \cdots & 0 \\ \vdots & \vdots & \vdots & \ddots & \vdots \\ \mathrm{Tr}(\tilde{A}_n^{k-1}) & \mathrm{Tr}(\tilde{A}_n^{k-2}) & \mathrm{Tr}(\tilde{A}_n^{k-3}) & \cdots & 1 \\ \mathrm{Tr}(\tilde{A}_n^{k}) & \mathrm{Tr}(\tilde{A}_n^{k-1}) & \mathrm{Tr}(\tilde{A}_n^{k-2}) & \cdots & \mathrm{Tr}(\tilde{A}_n) \end{pmatrix}.$$

Then, it is easy to show that

$$\begin{aligned} T_n^{(k)} &\to 0, \forall k \in I_{1,r} \Rightarrow \exists\, \mathrm{r\ MZMs}, \\ \left(T_n^{(k)} \right. &\to 0, \forall k \in I_{2,r}) \mathrm{or} \left(\frac{T_n^{(k)}}{T_n^{(1)}} \to 0, \forall k \in I_{2,r} \right) \\ &\Rightarrow \exists\, \mathrm{r\text{-}1\ MZMs}, \\ &\vdots \\ T_n^{(r)} &\to 0 \ \text{ or } \ \frac{T_n^{(r)}}{T_n^{(1)}} \to 0 \ \text{ or } \cdots \text{ or } \ \frac{T_n^{(r)}}{T_n^{(r-1)}} \to 0 \Rightarrow \exists\,, \end{aligned}$$

where $I_{i,j} = \{i, i+1, \cdots, j\}$. On the other hand, for $w_\ell \neq \Delta_\ell$, defining $T_n^{(k)} = \mathrm{Tr}(\bigwedge^k \tilde{\mathcal{A}}_n)$, we get the eigenvalue equation

$$\sum_{k=0}^{2r} (-1)^k \lambda_n^{2r-k} T_n^{(k)} = 0. \tag{C2}$$

In this case, the conditions are modified as follows:

$$\begin{aligned} T_n^{(k)} &\to 0, \forall k \in I_{1,2r} \Rightarrow v^< = 2r, \\ \left(T_n^{(k)} \right. &\to 0, \forall k \in I_{2,2r}) \mathrm{or} \left(\frac{T_n^{(k)}}{T_n^{(1)}} \to 0, \forall k \in I_{2,2r} \right) \\ &\Rightarrow v^< = 2r-1, \\ &\vdots \\ T_n^{(2r)} &\to 0 \ \text{ or } \ \frac{T_n^{(2r)}}{T_n^{(1)}} \to 0 \ \text{ or } \cdots \text{ or } \ \frac{T_n^{(2r)}}{T_n^{(2r-1)}} \to 0 \\ &\Rightarrow v^< = 1, \end{aligned}$$

otherwise $v^< = 0$. After defining

$$T'^{(k)}_n = \frac{T_n^{(2r-k)}}{T_n^{(2r)}}, \tag{C3}$$

we get similar conditions for $v^>$, which read

$$\begin{aligned} T'^{(k)}_n &\to 0, \forall k \in I_{1,2r} \Rightarrow v^> = 2r, \\ &\left(T'^{(k)}_n \to 0, \forall k \in I_{2,2r}\right) \mathrm{or} \left(\frac{T'^{(k)}_n}{T'^{(1)}_n} \to 0, \forall k \in I_{2,2r} \right) \\ &\Rightarrow v^> = 2r-1, \\ &\vdots \\ T'^{(2r)}_n &\to 0 \ \text{ or } \ \frac{T'^{(2r)}_n}{T'^{(1)}_n} \to 0 \ \text{ or } \cdots \text{ or } \ \frac{T'^{(2r)}_n}{T'^{(2r-1)}_n} \to 0 \\ &\Rightarrow v^> = 1, \end{aligned}$$

otherwise $v^> = 0$. We then obtain the number of MZMs which is given by $\max(v^<, v^>) - r$, where typically $v^> = 2r - v^<$.

APPENDIX D: CALCULATION OF THE SELF-ENERGY

We write $H_0 = \sum_{m,n} c_m \mathcal{H}_{mn} c_n$, where $i\mathcal{H}$ is the real and skew-symmetric matrix

$$\begin{aligned} \mathcal{H} = \sum_{i,j} |i\rangle\langle j| \otimes \mathcal{H}_{i,j} &= \sum_j |j\rangle\langle j| \otimes \mathcal{H}_0 \\ &+ \sum_j \sum_\ell |j\rangle\langle j+\ell| \otimes \mathcal{H}_\ell + |j+\ell\rangle\langle j| \otimes (\mathcal{H}_\ell)^\dagger, \end{aligned} \tag{D1}$$

where $\mathcal{H}_0$ and $\mathcal{H}_\ell$ are the matrices $\mathcal{H}_0 = \mu\tau_2/4$ and $\mathcal{H}_\ell = w\ell^{-\alpha}\tau_2/4 + i\Delta\ell^{-\beta}\tau_1/4$, where the nth component of $|i\rangle$ is $(|i\rangle)_n = \delta_{n,i}$. We consider periodic boundary conditions, and we change the basis by defining the vectors $|k\rangle$ such that $|j\rangle = \sum_k e^{-ikj}|k\rangle/\sqrt{L}$. We can then write $\mathcal{H} = \sum_k |k\rangle\langle k| \otimes \mathcal{H}(k)$, where $\mathcal{H}(k) = ((\mu + wg(k))\tau_2 - \Delta f(k)\tau_1)/4$. The inverse of the matrix $\mathcal{H}$ reads

$$(\mathcal{H})^{-1} = -4i \sum_k |k\rangle\langle k| \otimes \begin{pmatrix} 0 & 1/X_+ \\ -1/X_- & 0 \end{pmatrix}, \tag{D2}$$

where $X_\pm = \mu + wg(k) \pm i\Delta f(k)$. We now add a disorder term $H_1 = -\sum_{j=1}^L \omega_j n_j$ to the Hamiltonian H_0, where $\omega_j = \mu_j - \mu$, corresponding to the matrix $\mathcal{H}_1 = \sum_i \omega_i |i\rangle\langle i| \otimes \tau_2/4$. For $E = 0$, we get $\mathcal{G}_0 = -(\mathcal{H})^{-1}$, and the self-energy $\Sigma' \approx \langle \mathcal{H}_1 \mathcal{G}_0 \mathcal{H}_1 \rangle$ reads

$$\begin{aligned} \Sigma' \approx \frac{\delta\mu}{4} \sum_{j=1}^L |j\rangle\langle j| \otimes \tau_2 + \sum_j \sum_\ell |j\rangle\langle j \\ + \ell| \otimes \Sigma'_\ell + |j+\ell\rangle\langle j| \otimes (\Sigma'_\ell)^\dagger \end{aligned} \tag{D3}$$

with $\Sigma'_\ell = \delta w_\ell \tau_2/4 + i\delta\Delta_\ell\tau_1/4$, where $\delta\mu$, δw_ℓ, and $\delta\Delta_\ell$ given by Eqs. (76)–(78), from which we get the self-energy Σ in terms of Majorana operators reported in Eq. (75).

[1] A. P. Schnyder, S. Ryu, A. Furusaki, and A. W. W. Ludwig, Phys. Rev. B **78**, 195125 (2008).
[2] A. Kitaev, AIP Conf. Proc. **1134**, 22 (2009).
[3] A. Yu. Kitaev, Ann. Phys. **303**, 2 (2003).
[4] S. Nadj-Perge, I. K. Drozdov, J. Li, H. Chen, S. Jeon, J. Seo, A. H. MacDonald, B. A. Bernevig, and A. Yazdani, Science **346**, 602 (2014).
[5] R. Pawlak, M. Kisiel, J. Klinovaja, T. Meier, S. Kawai, T. Glatzel, D. Loss, and E. Meyer, npj Quantum Inf. **2**, 16035 (2016).
[6] M. Ruby, B. W. Heinrich, Y. Peng, F. von Oppen, and K. J. Franke, Nano Lett. **17**, 4473 (2017).
[7] J. D. Sau, S. Tewari, R. M. Lutchyn, T. D. Stanescu, and S. Das Sarma, Phys. Rev. B **82**, 214509 (2010).
[8] Y. Oreg, G. Refael, and F. von Oppen, Phys. Rev. Lett. **105**, 177002 (2010).
[9] J. Alicea, Phys. Rev. B **81**, 125318 (2010).
[10] V. Mourik, K. Zuo, S. M. Frolov, S. Plissard, E. Bakkers, and L. Kouwenhoven, Science **336**, 1003 (2012).
[11] J. Alicea, Y. Oreg, G. Refael, F. Von Oppen, and M. P. A. Fisher, Nat. Phys. **7**, 412 (2011).
[12] A. R. Akhmerov, Phys. Rev. B **82**, 020509(R) (2010).
[13] D. Vodola, L. Lepori, E. Ercolessi, A. V. Gorshkov, and G. Pupillo, Phys. Rev. Lett. **113**, 156402 (2014).
[14] A. Alecce and L. Dell'Anna, Phys. Rev. B **95**, 195160 (2017).
[15] K. Patrick, T. Neupert, and J. K. Pachos, Phys. Rev. Lett. **118**, 267002 (2017).
[16] L. Lepori and L. Dell'Anna, New J. Phys. **19**, 103030 (2017).
[17] Z. Gong, T. Guaita, and J. I. Cirac, Phys. Rev. Lett. **130**, 070401 (2023).
[18] N. G. Jones, R. Thorngren, and R. Verresen, arXiv:2211.15690.
[19] O. Motrunich, K. Damle, and D. A. Huse, Phys. Rev. B **63**, 224204 (2001).
[20] P. W. Brouwer, M. Duckheim, A. Romito, and F. von Oppen, Phys. Rev. Lett. **107**, 196804 (2011).
[21] W. DeGottardi, D. Sen, and S. Vishveshwara, Phys. Rev. Lett. **110**, 146404 (2013).
[22] X. Cai, L.-J. Lang, S. Chen, and Y. Wang, Phys. Rev. Lett. **110**, 176403 (2013).
[23] W. DeGottardi, M. Thakurathi, S. Vishveshwara, and D. Sen, Phys. Rev. B **88**, 165111 (2013).
[24] N. M. Gergs, L. Fritz, and D. Schuricht, Phys. Rev. B **93**, 075129 (2016).
[25] A. Nava, R. Giuliano, G. Campagnano, and D. Giuliano, Phys. Rev. B **95**, 155449 (2017).
[26] S. Lieu, D. K. K. Lee, and J. Knolle, Phys. Rev. B **98**, 134507 (2018).
[27] A. Habibi, S. A. Jafari, and S. Rouhani, Phys. Rev. B **98**, 035142 (2018).
[28] C. Monthus, J. Phys. A: Math. Theor. **51**, 465301 (2018).
[29] C. Monthus, J. Phys. A: Math. Theor. **51**, 115304 (2018).
[30] C.-B. Hua, R. Chen, D.-H. Xu, and B. Zhou, Phys. Rev. B **100**, 205302 (2019).
[31] H.-Y. Hui, J. D. Sau, and S. Das Sarma, Phys. Rev. B **90**, 064516 (2014).
[32] A. M. Lobos, R. M. Lutchyn, and S. Das Sarma, Phys. Rev. Lett. **109**, 146403 (2012).
[33] R. Thomale, S. Rachel, and P. Schmitteckert, Phys. Rev. B **88**, 161103(R) (2013).
[34] M. McGinley, J. Knolle, and A. Nunnenkamp, Phys. Rev. B **96**, 241113(R) (2017).
[35] G. Kells, N. Moran, and D. Meidan, Phys. Rev. B **97**, 085425 (2018).
[36] J. Wouters, H. Katsura, and D. Schuricht, Phys. Rev. B **98**, 155119 (2018).
[37] P. W. Brouwer, M. Duckheim, A. Romito, and F. von Oppen, Phys. Rev. B **84**, 144526 (2011).
[38] R. M. Lutchyn, T. D. Stanescu, and S. Das Sarma, Phys. Rev. Lett. **106**, 127001 (2011).
[39] A. R. Akhmerov, J. P. Dahlhaus, F. Hassler, M. Wimmer, and C. W. J. Beenakker, Phys. Rev. Lett. **106**, 057001 (2011).
[40] J. D. Sau, S. Tewari, and S. Das Sarma, Phys. Rev. B **85**, 064512 (2012).
[41] J. Liu, A. C. Potter, K. T. Law, and P. A. Lee, Phys. Rev. Lett. **109**, 267002 (2012).
[42] H.-Y. Hui, J. D. Sau, and S. Das Sarma, Phys. Rev. B **92**, 174512 (2015).
[43] J. D. Sau and S. Das Sarma, Phys. Rev. B **88**, 064506 (2013).
[44] C.-X. Liu, J. D. Sau, T. D. Stanescu, and S. Das Sarma, Phys. Rev. B **96**, 075161 (2017).
[45] A. Haim and A. Stern, Phys. Rev. Lett. **122**, 126801 (2019).
[46] H. Pan, J. D. Sau, and S. Das Sarma, Phys. Rev. B **103**, 014513 (2021).
[47] A. M. Cook, M. M. Vazifeh, and M. Franz, Phys. Rev. B **86**, 155431 (2012).
[48] P. Zhang, and F. Nori, New J. Phys. **18**, 043033 (2016).
[49] H. Pan and S. Das Sarma, Phys. Rev. Res. **2**, 013377 (2020).
[50] H. Pan and S. Das Sarma, Phys. Rev. B **103**, 224505 (2021).
[51] H. Pan and S. Das Sarma, Phys. Rev. B **105**, 115432 (2022).
[52] S. Ahn, H. Pan, B. Woods, T. D. Stanescu, and S. Das Sarma, Phys. Rev. Mater. **5**, 124602 (2021).
[53] W. S. Cole, J. D. Sau, and S. Das Sarma, Phys. Rev. B **94**, 140505(R) (2016).
[54] O. A. Awoga, K. Björnson, and A. M. Black-Schaffer, Phys. Rev. B **95**, 184511 (2017).
[55] D. E. Liu, E. Rossi, and R. M. Lutchyn, Phys. Rev. B **97**, 161408(R) (2018).
[56] L.-L. Zhu, Q. Huang, H.-L. Dai, C. Kong, Y. Feng, and C.-J. Shan, Laser Phys. Lett. **12**, 015202 (2015).
[57] X. Cai, J. Phys.: Condens. Matter **29**, 115401 (2017).
[58] M.-T. Rieder, G. Kells, M. Duckheim, D. Meidan, and P. W. Brouwer, Phys. Rev. B **86**, 125423 (2012).
[59] M.-T. Rieder, P. W. Brouwer, and İ. Adagideli, Phys. Rev. B **88**, 060509(R) (2013).
[60] M.-T. Rieder and P. W. Brouwer, Phys. Rev. B **90**, 205404 (2014).
[61] A. Altland, D. Bagrets, L. Fritz, A. Kamenev, and H. Schmiedt, Phys. Rev. Lett. **112**, 206602 (2014).
[62] B. Pekerten, A. Teker, Ö. Bozat, M. Wimmer, and İ. Adagideli, Phys. Rev. B **95**, 064507 (2017).
[63] İ. Adagideli, M. Wimmer, and A. Teker, Phys. Rev. B **89**, 144506 (2014).

[64] J. J. He, J. Wu, T.-P. Choy, X-J. Liu, Y. Tanaka, and K. T. Law, Nat. Commun. **5**, 3232 (2014).
[65] G. Francica and L. Dell'Anna, Phys. Rev. B **106**, 155126 (2022).
[66] S. B. Jäger, L. Dell'Anna, and G. Morigi, Phys. Rev. B **102**, 035152 (2020).
[67] E. Ott, *Chaos in Dynamical Systems* (Cambridge University Press, Cambridge, UK, 1993).
[68] V. Loreto, G. Paladin, M. Pasquini, and A. Vulpiani, Physica A **232**, 189 (1996).
[69] J. F. Paydon and H. S. Wall, Duke Math. J. **9**, 360 (1942).
[70] T. A. Loring, Ann. Phys. **356**, 383 (2015).